Research Article

Structural behavior of historical Obruk Inn under different earthquakes

Süleyman Kamil Akın [a,*], Ahmet Alagöz [a]

[a] *Department of Civil Engineering, KTO Karatay University, 42020 Karatay, Konya, Türkiye*

ABSTRACT

Masonry structures is one of the most preferred structure types throughout history. The advantageous of these structures can be categorized as longevity, affordability and easy access to materials. Due to a lack of information and constructive errors, masonry structures suffer major damage under effect of earthquakes. While the vertical load carrying capacity of a masonry structure is excellent, its performance under horizontal loads is very poor. The brittle behavior of masonry structures, in particular, causes the structure to suffer significant damage or collapse completely during an earthquake. Türkiye is situated over a major earthquake zone. Throughout history, there has been numerous major earthquakes. These earthquakes have demolished the masonry structures resulted in significant life and economic losses. Therefore, in recent days, the examination of the seismic resilience performance of masonry structures as well as the required strengthening have become a pivotal issue. Thus, the aim of this study is to analyze the seismic performance of historical Obruk Inn subjected to different earthquake effects via finite elements method (FEM). To do this, the plans obtained from on-site inspections for historical Obruk Inn to create structural FEM model and its performance was evaluated under the influence of various earthquake excitations. As a result of the analyses, it was determined that the historical Obruk Inn structure should have immediate be strengthened against a possible earthquake.

ARTICLE INFO

Article history:
Received 19 December 2023
Revised 8 January 2024
Accepted 23 February 2024

Keywords:
Masonry structures
Finite element method
Earthquake performance
Historical structure

1. Introduction

Masonry structures are among the oldest types of structures that have been used throughout history (Kamal et al. 2014). As a result, the majority of masonry structures are historically significant but still in use (Gattesco et al. 2014). These structures have numerous advantages, including low cost, durability, and longevity (Hamid, 2006). Accordingly, the vast majority of building stock in Pakistan (93 percent), Mexico (76%), Peru (73%), and Italy (62%) is comprised of masonry building structures, including both existing and modern structures (Aşıkoğlu et al. 2020). The ability to pass through wide openings without columns, particularly thanks to the dome system, made it very popular in the construction of structures such as palaces and mosques during the Islamic period (Hejazi el al. 2015, and Hejazi et al. 2021). Therefore, Türkiye has a large number of historical masonry structures. Easy access to materials, particularly in rural areas, leads to greater preference. Moreover, masonry structures have many disadvantages as well as their advantages. While masonry structures can safely bear vertical loads thanks to rigid wall elements, their performance under horizontal dynamic loads, such as earthquakes, is poor (Pauletta et al. 2017). The complex structural configuration of masonry structures, as well as insufficient and incomplete knowledge of their structural systems, has a significant impact on the earthquake behavior of stacking structures (Asteris et al. 2014). Most countries have masonry structures that have manufacturing defects or have not received the required engineering service. These structures are exosed

* *Corresponding author*. Tel.: +90-444-1-251 ; E-mail address: kamil.akin@karatay.edu.tr (S. K. Akın)
ISSN: 2149-8024 / DOI: https://doi.org/10.20528/cjsmec.2024.01.004

to numerous horizontal load cycles during earthquakes causing great damage or collapse during a severe earthquake (Kollerathu et al. 2017). The poor earthquake performance of masonry structures, on the other hand, leads significant life and economic losses (Bruneau 1994; Tomazevic 1999). Hence not only in Türkiye, but also in all over the world the strengthening of masonry structures is required. One of the most important reasons for these amendments is the wear of the masonry structure due to time-dependent effects, the changing loading conditions due to unconscious modifications and changes in usage (Akcay et al. 2016). It is critical to determine the accurate seismic performance of masonry structures and to ensure the necessity of strengthening.

Anatolia is located on trade routes, many caravanserais were built, more specifically during the Anatolian Seljuk Period. Historical Obruk Inn Caravanserai is one of them. These structures, which were built at a distance of about 30-40 kilometers apart, were constructed to meet the needs of trade caravan groups. The Anatolian Seljuks used a plan scheme with closed and open courtyards to construct it. The historical Obruk Inn's entrance is to the west, and its facade is reminiscent of a castle, as shown in Fig. 1.

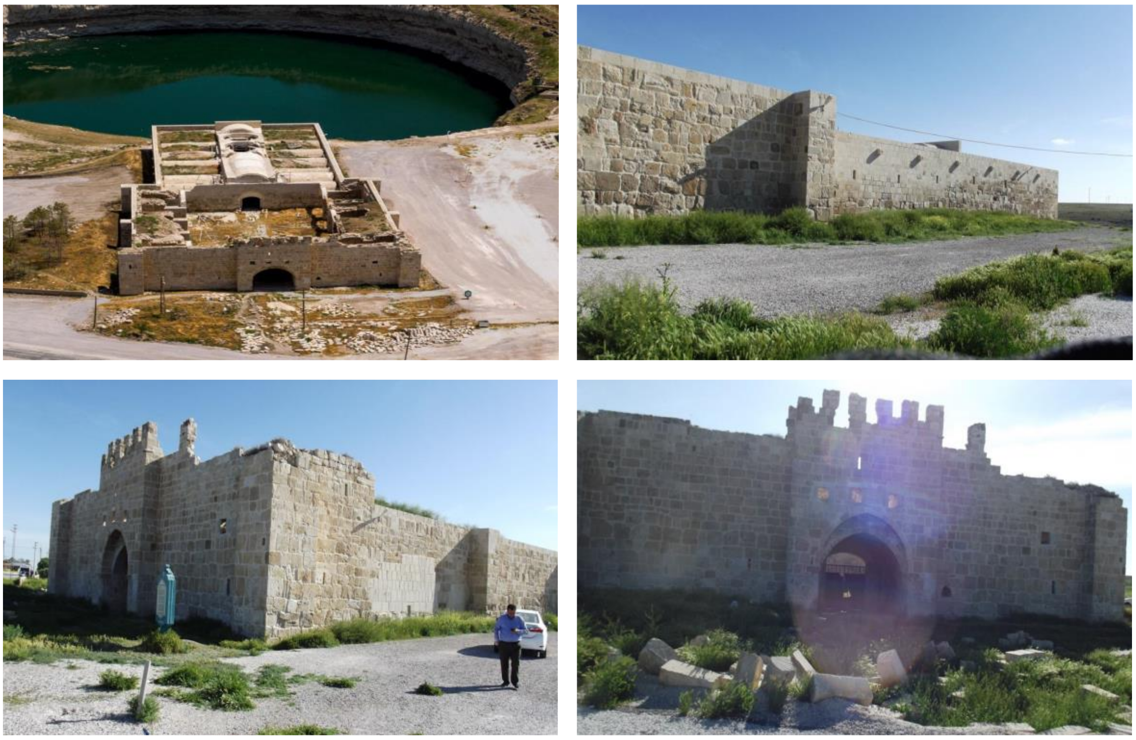

Fig. 1. Historical Obruk Inn.

It's located at the entrance to Obruk Village. It is right beside the Obruk Lake, which is also known as "Kızören Obruğu." (Fig. 2).

Faced stone, undressed stone and various spolia antique materials were used in its construction. The west facade, which houses the inn's entrance have two stories tall, while the other facades have single stories. Separate space arrangements were made on the second floor, and the masjid was also located here. Fig. 3 shows the building's ground, first and roof plans.

Modelling of structures and performing dynamic static analyses with the finite element method (FEM) is an extremely useful method for determining the causes of structural damage (Laefer et al. 2014; Tomaszewska 2010; Tomaszewska et al. 2012; Grillanda et al. 2019; Kujawa et al. 2020). Many studies are being conducted today to determine the earthquake behavior of masonry structures throughout FEM analysis (Asteris et al. 2014; Abruzzese et al. 2009; D'Agostino et al. 2009; Uzun et al. 2018; Sandoli et al. 2020, Theodossopoulos et al. 2013). In this study, the historical Obruk Inn's performance under the influence of different earthquake loads was investigated over SAP2000 structural analysis program.

At the present stage of knowledge, numerical simulations are fundamental to provide insight into the structural behavior and support the derivation of rational design rules but nonlinear finite element analyses will be always helpful for the validation of the design of complex masonry structures under complex loading conditions. In particular, computations beyond the limit load down to a possibly lower residual load are needed to assess the safety of the structure. Aside from failure analysis, also the serviceability limit states can be successfully validated with numerical analyses. FEM is a useful, reliable and valid tool for design and modelling of new and existing structures.

Another important aspect is the safety of existing structures under existing or new loading conditions, with an emphasis in the preservation of historical structures.

Reliable numerical models are necessary to assess and strengthen existing masonry structures. The final point is the need to improve the performance of masonry buildings in underdeveloped countries.

Fig. 2. Location of Historical Obruk Inn.

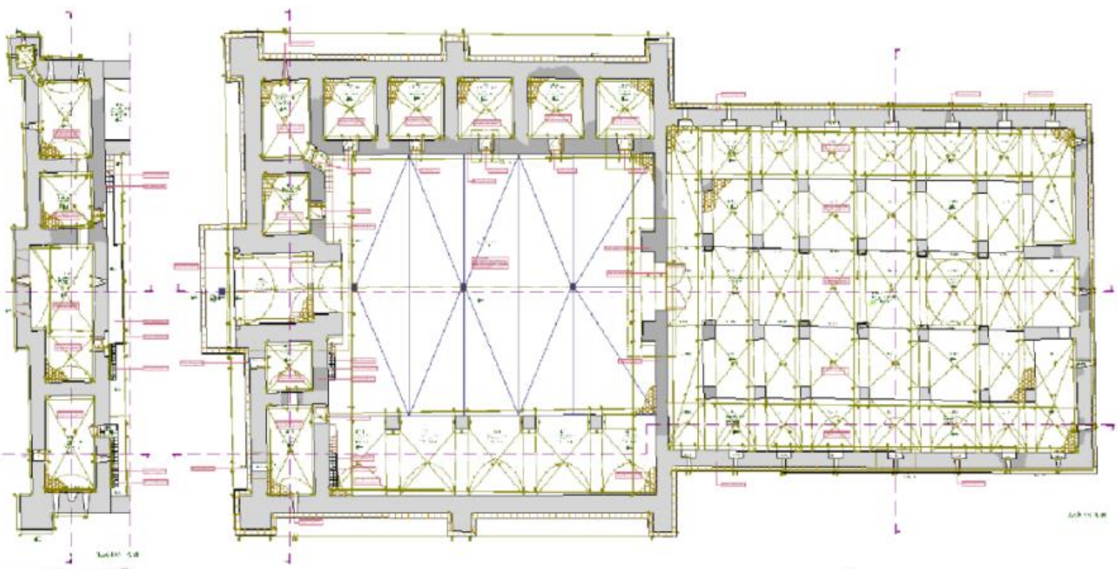

(a)

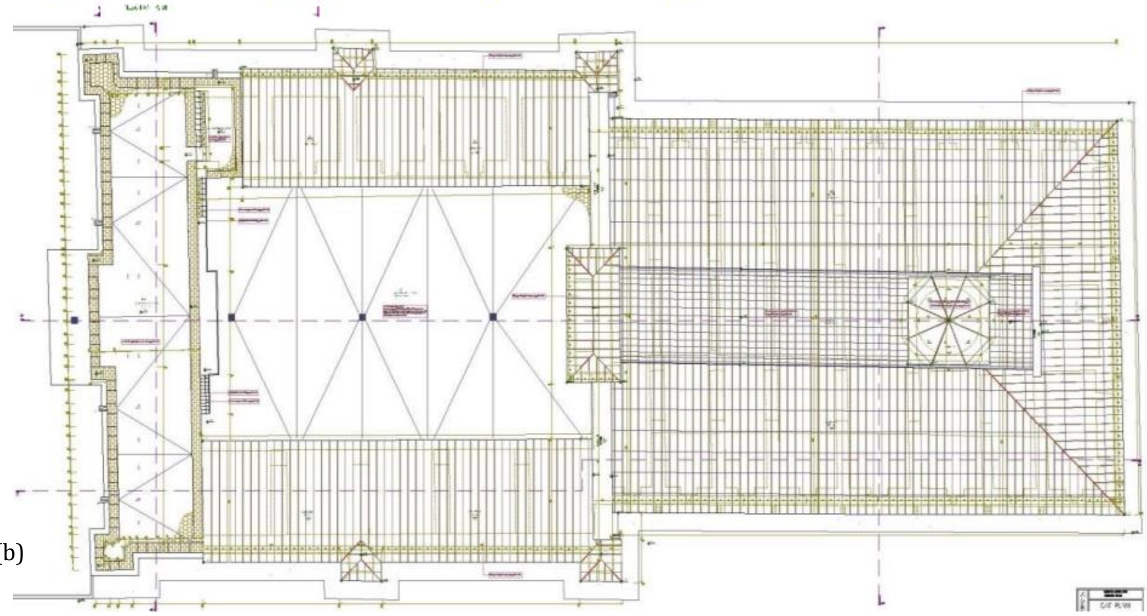

(b)

Fig. 3. Historical Obruk Inn: (a) Ground floor plan, (b) Roof floor plan.

2. Materials and method

2.1. Approaches to modeling of masonry structures

The modeling and evaluation of structures represent the most contentious issue among design engineers (Cakir 2022). Many studies had been made according to the modelling of unreinforced masonry structures. Evaluation of load carrying capacity of this type of structures usually needs to characterize the mechanical properties of the elements. For this reason, at first, the mechanical properties of constitutive materials including, bricks, adobes, mortars, pier elements of adobe and a vault element of brick were determined using standard experimental tests. Strength of a masonry building depends on both the bond between brick and mortar (Ahmadzai et al. 2022; Karaton and Çanakçı 2021). The results of samples tested, reconfirmed the very low tensile bond strength to be expected of masonry elements, emphasizing the inability of these types of materials to resist a tensile force. Finally, the mechanical properties of pier and vault testing samples were implemented in a nonlinear finite element (FE) analysis of the building, under lateral loading, through macro-modelling concepts (Eslami et al. 2012).

Masonry structures have a heterogeneous structural configuration made out of many dissimilar parts. These are wall material and mortar as binding material (Klinger 2010). Masonry structures typically have high weight, low tensile and shear strength, and behave brittle. The FEM is commonly used to perform numerical analyses for masonry structures. For this aim, firstly, the structure's finite element model should be created (Kamal et al. 2014). Vertical, horizontal, and rigid elements interactions between materials should be modelled correctly (Petrovčič et al. 2013). Additionally, the seismic behavior of masonry structures in general has been known for years. Geometry of structure, rigidity of horizontal and vertical elements to support the structure are the factors that affects the behavior of structure (Milani et al. 2017). For this reason, a number of modeling techniques are employed to reflect the behavior of the masonry construction. The Fig. 4 depicts these modeling techniques (Lourenço 1996).

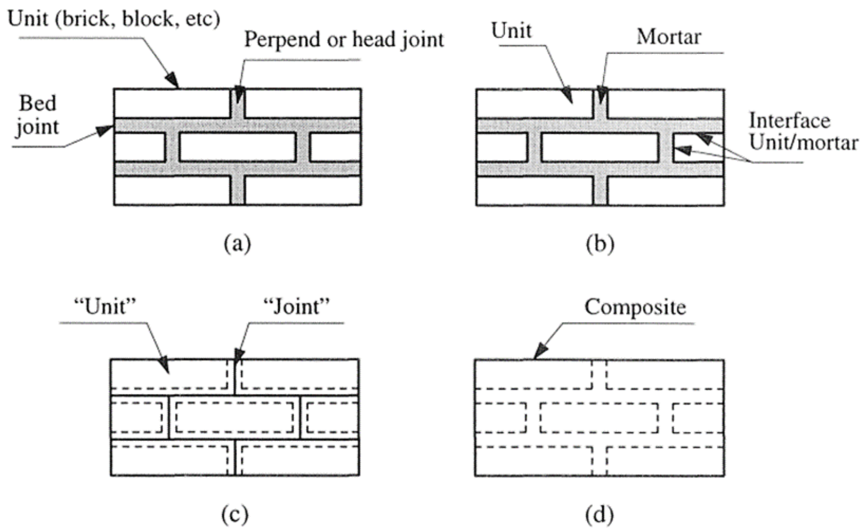

Fig. 4. Modelling methods for masonry structures: (a) Masonry sample; (b) Detailed micro-modeling; (c) Simplified micro-modeling; (d) Macro-modeling (Lourenço 1996).

2.1.1. Detailed micro modeling

In this case, masonry units and mortar joints are modeled as a continuum separately. In addition, as shown in Fig. 4a, a discontinuous interface is defined on the surface between the masonry units and the mortar joints. This type of modeling takes a lot of effort, but better results can be obtained. In scientific studies, this sort of modeling is widely preferred (Giordano et al.2017).

2.1.2. Simplified micro modeling

Without modeling the discontinuous interface between the mortar joint and the masonry structural unit, the bond between the mortar and the masonry structural unit is represented by continuous elements. This type of modeling is given in Fig. 4b.

2.1.3. Macro modeling

It is the simplest type of modeling. In this modeling technique, the mortar joints, masonry units, and unit/mortar interface are represented by continuum elements (Lourenço 1996). This type of modeling is given in Fig. 4c. This type of modeling is the most applicable modeling method. Especially in structures with long walls, a more uniform distribution of stresses is achieved (Chen et al. 2018).

2.2. Material properties

The building's structural system materials (inner and outer walls, as well as materials used in the vaults) were treated as two separate materials in the building model. The material properties mentioned in Table 1 are determined according to TEC-2007 (2007).

Table 1. Material properties.

Material	Modulus of elasticity (MPa)	Unit weight of bulk (kN/m^3)	Poisson's ratio
Mortar + stone	4500	24	0.20
Vaults	4000	18	0.18

2.3. Establishing the building model

In accordance with the actual building dimensions, the historical Obruk Inn was modeled in the SAP2000 structural analysis program. For modeling, the material properties listed in Table 1 were used. The building's walls are modeled as shell elements. The building's columns are modeled as rod elements. For stone and mortar, a homogeneous single material property was used for considering the macro modeling method. Fig. 5 depicts the building's three-dimensional model.

In the numerical model created, G1 is defined as a dead load, G2 as additional load, and Q as live load (snow load). Earthquake loads were applied to the system in X and Y directions as equivalent earthquake loads. EXP and EYP are defined as positive earthquake loads as well as EXN and EYN are defined as negative earthquake loads. In accordance with the earthquake code TEC-2007 (2007), the 5% eccentric effect was taken into account. The soil class of the region is Z3 according to TEC-2007 (2007). The building is located in the 5th degree earthquake zone. The building importance factor (coefficient) (I) has been taken as 1, and the earthquake load reduction coefficient (R), has been taken as 2 in line with the value determined by the Earthquake Code for masonry structures (TEC-2007). G2 additional loads were computed separately, taking into account the filling material used in the building, and live loads were taken in accordance with the earthquake code. Because the height of the area where the building is located is around 1000 meters above sea level, the snow load was determined as 0.8 $kN\backslash m^2$ according to TS 498. Since the roof covering in closed area will be a lead plate (3 mm), the coating load has also been taken into account in the calculations. According to the rule that the total effective mass of the building should not be less than 90% of the total mass of the building, it is seen that the mass participation ratios in the x, y and z directions of the building exceed 90% in the last mode (Table 2).

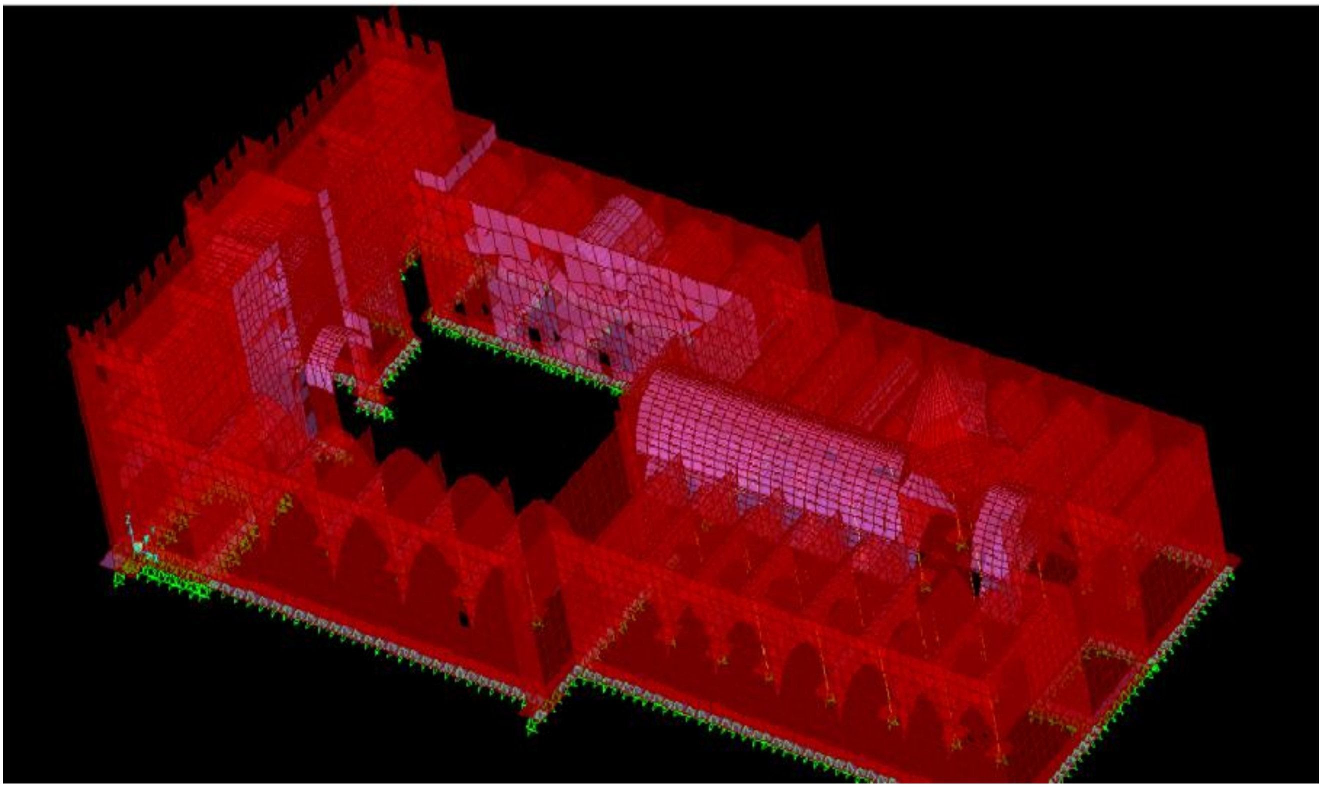

Fig. 5. Three-dimensional model of the structure.

The safe stresses for the materials were obtained by using the safety stress values for the materials with unknown unconfined compressive strength in the TEC-2007 (2007) code. The values defined in the code are listed in Table 3.

Table 2. Mass participation ratios and period.

Mode	Period (s)	Mass participation ratio UX (%)	Mass participation ratio UY (%)	Mass participation ratio UZ (%)
1	0.271344	0.00008104	0.05900	0.000004632
2	0.258326	0.00525	0.22931	0.00011
3	0.254005	0.20487	0.23524	0.00015
4	0.248451	0.20490	0.24469	0.00015
5	0.238386	0.21068	0.24471	0.00016
6	0.233619	0.21693	0.24576	0.00095
7	0.228081	0.21825	0.24882	0.00128
8	0.221302	0.22415	0.29566	0.00148
9	0.212641	0.23762	0.29639	0.00159
10	0.208915	0.26444	0.29639	0.00160
11	0.197601	0.27383	0.29668	0.00162
12	0.193502	0.27507	0.29668	0.00162
13	0.181558	0.27582	0.29671	0.00170
14	0.174658	0.28433	0.29673	0.00170
15	0.169962	0.28438	0.30109	0.00182
16	0.168491	0.28594	0.30609	0.00186
17	0.165680	0.35395	0.30650	0.00209
18	0.164603	0.38076	0.30656	0.00219
19	0.156734	0.38402	0.35651	0.00221
20	0.153036	0.38433	0.36416	0.00223
21	0.144948	0.38854	0.37368	0.00230
22	0.140602	0.39566	0.44897	0.00240
23	0.137722	0.54390	0.44940	0.00269
24	0.130412	0.55413	0.44997	0.00527
25	0.124780	0.55675	0.47982	0.00626
26	0.104597	0.55895	0.71655	0.00660
27	0.101820	0.56264	0.71684	0.01502
28	0.096905	0.56321	0.71735	0.05952
29	0.095192	0.56899	0.77423	0.06477
30	0.092200	0.58062	0.78328	0.08887
31	0.086529	0.66449	0.78522	0.09462
32	0.070033	0.66450	0.78647	0.17443
33	0.064365	0.66450	0.78647	0.21715
34	0.062405	0.66590	0.78650	0.33385
35	0.051892	0.67263	0.84691	0.33412
36	0.047345	0.68430	0.90480	0.33538
37	0.045430	0.90010	0.90509	0.33663
38	0.038496	0.90089	0.90629	0.55574
39	0.033089	0.90102	0.91253	0.57279
40	0.030616	0.90244	0.91484	0.90166

Table 3. Compressive safety stresses of walls with unknown unconfined compressive strength (TEC-2007).

Type of masonry unit used in the wall	Mortar wall pressure safety stress, f_{em} (MPa)
Vertically perforated block brick (with less than 35% cement-reinforced lime mortar)	1.0
Vertically perforated block brick (hole rate between 35-45%, with cement-reinforced lime mortar)	0.8
Vertically perforated block brick (with a cement-reinforced lime mortar with a hole rate of more than 45%)	0.5
Solid block brick or Blending brick (with cement-reinforced lime mortar)	0.8
Stone wall (with cement-reinforced lime mortar)	0.3
Aerated concrete (with adhesive)	0.6
Solid concrete briquette (with cement mortar)	0.8

The compression safety stress for stone masonry walls f_{em}=0.3 MPa and the compression safety stress for briquette masonry walls is f_{em}=0.8. On the other hand, the safety stresses are magnified by a factor of 3. In this case, the bearing stress for stone wall was assumed as $f_{em,b}$=0.3×3=0.9 MPa, and bearing stress for brick wall was assumed as $f_{em,b}$=0.8×3=2.4 MPa. Tensile stresses can be accepted as 15% of the value determined as compressive safety stress. In this case, the tensile safety stress for the stone wall was assumed as; $f_{em,ç}$=0.9×0.15=0.135 MPa and tensile stress for brick walls was assumed as; $f_{em,ç}$=2.4×0.15=0.36 MPa. The compressive and tensile stresses of the mentioned materials are given in Table 4.

Table 4. Acceptable safety stresses for materials.

Material	Compressive safety stress (MPa)	Tensile safety stress (MPa)
Brick (with mortar)	2.40	0.360
Stone wall (with mortar)	0.90	0.135

In order to apply the earthquake load effect to the structure, three different earthquake acceleration records were applied to the structure with the Time History Analysis Method. The characteristic features of the applied earthquakes are given in Table 5. The main reason to select those seismic records is that they have various effective magnitudes and different ground speeds as well as their seismic characterizations differ in regarded to ground accelerations and focal lengths. The earthquake acceleration records for each earthquake are given in Fig. 6.

Table 5. Characteristics of applied earthquakes.

Earthquake record	Date	Magnitude	Ground speed (cm/s)	Ground acceleration (g)	Focal length (km)	Type of earthquake
Kocaeli	08/17/99	7.51	58.85	0.312	13.60	Strike-slip
Landers	06/28/92	7.28	29.60	0.152	23.62	Strike-slip
Taiwan	08/21/99	6.20	14.63	0.132	12.44	Strike-slip

3. Results and Discussion

Analyses were run in the SAP2000 program using the parameters from the historical Obruk Inn. As a result, Fig. 7 depicts the distribution of maximum stresses under G+Q loading in the overall view of the structure. Tensile stresses exceeding the predicted tensile safety stress for the material were observed in the left part of the building's west facade as a result of the G+Q loading combination (Fig. 7a). Horizontal stresses on the front facade reach up to 0.540 MPa ($f_{em,ç}$=0.135 MPa) values. Although such high stresses are not seen intensively at the main entrance of the structure, they increase the expectation that crack-like deformations may occur in some areas. Indeed, joint gaps and cracks have formed on the western front (Fig. 7b).

Base shear forces and displacements differ according to the geometry of the structure and acceleration. Different soil conditions should be studied also in further studies.

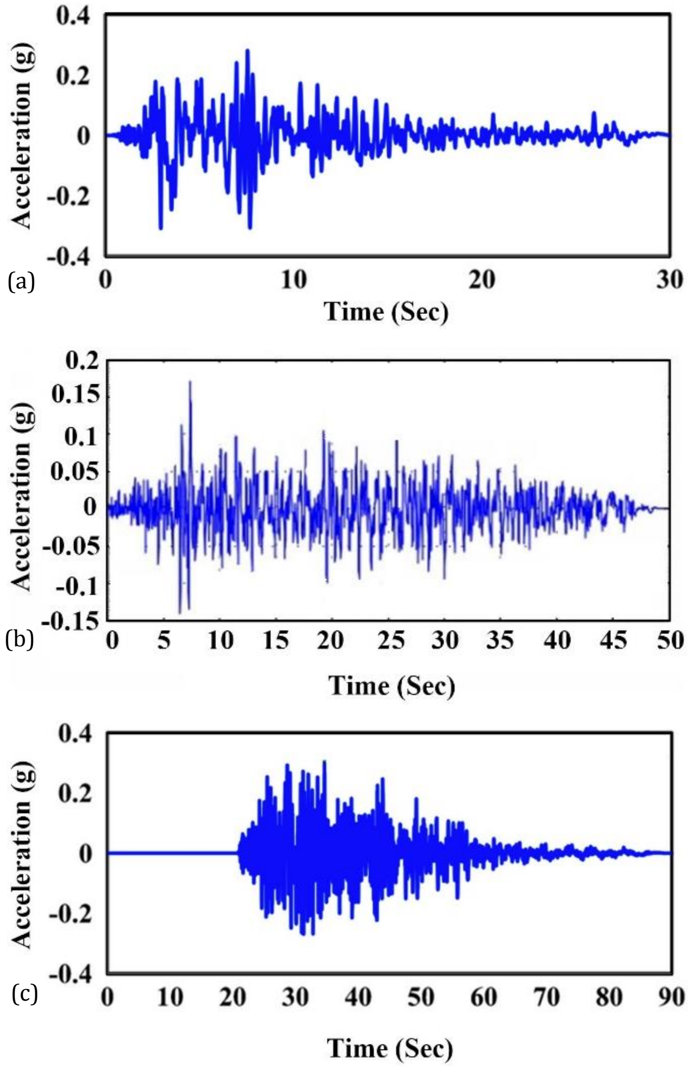

Fig. 6. Earthquake acceleration records: (a) Kocaeli; (b) Landers; (c) Taiwan.

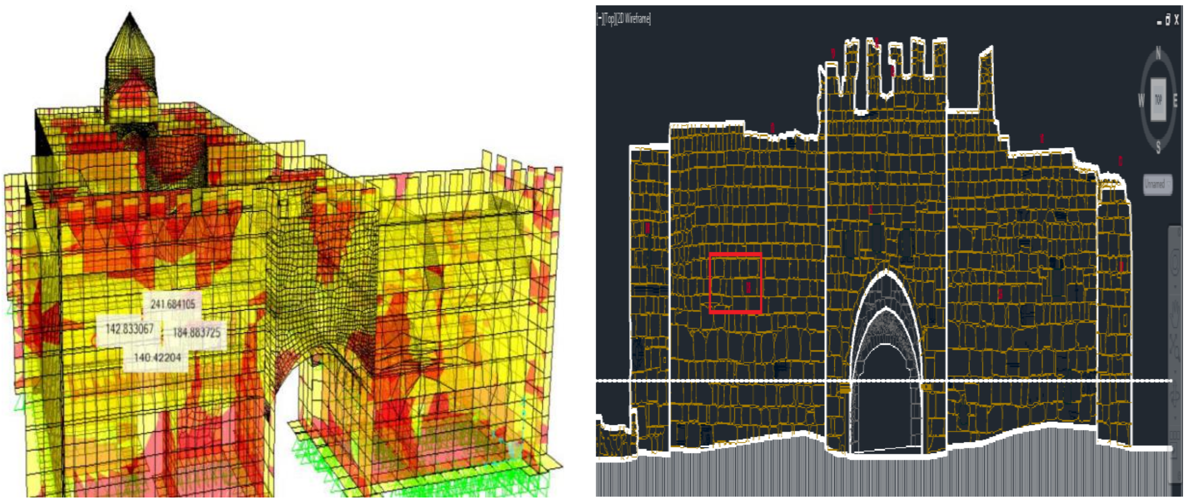

(a) (b)

Fig. 7. Historical Obruk Inn: (a) West facade maximum stress distribution under vertical loads; (b) West facade laser scanning result.

The examination of the building's eastern facade, as shown in Fig. 8, revealed that the tensile stresses in the horizontal direction reached up to 0.368 MPa value. As the stress value exceeded the tensile safety stress predicted for the material, joint gaps and dilatations occurred as a result of cracks at the points shown in the laser scanning of this facade, as shown in Fig. 8b, and this problem was resolved with new materials.

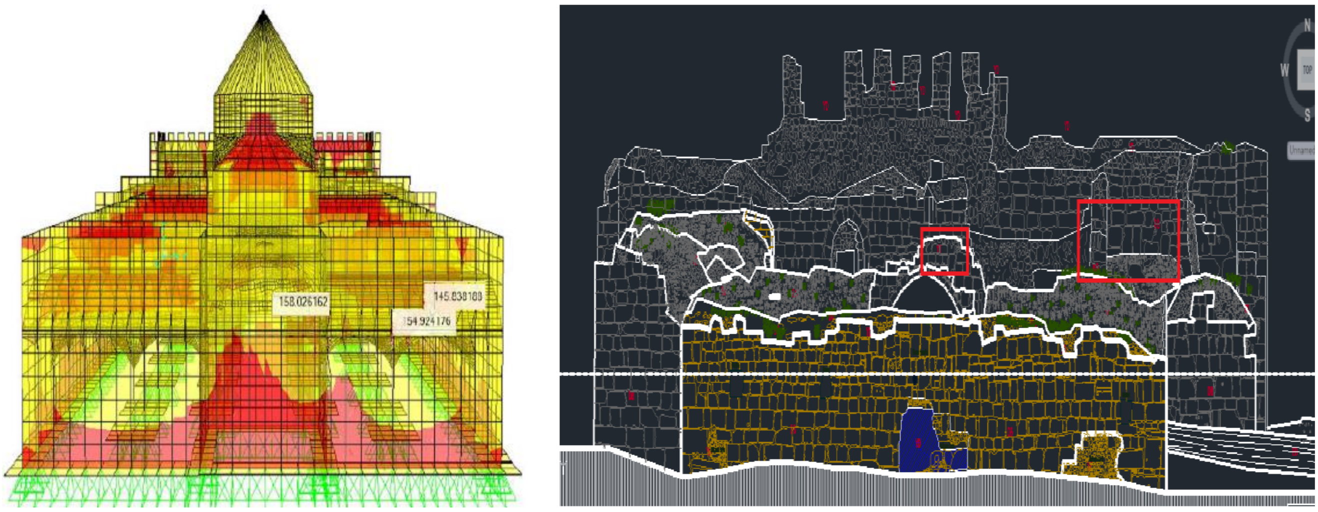

(a) (b)

Fig. 8. Historical Obruk Inn: (a) East facade maximum stress distribution under vertical loads; (b) East facade laser scanning result.

It was observed that the stresses in the open and closed volumes of the structure's south façade reached up to 0.463 MPa (Fig. 9a and Fig. 9c). These stresses are increasing in particular along the line where the vault arches of the structure connected to the outer wall. These stresses resulted in dilatations as a result of cracks in the middle section of façade which was repaired with new materials (Fig. 9b). The shape of the southern façade of the building created by laser scanning prior to restoration demonstrated the damage caused to the structure by the stresses that occurred in these areas (Fig. 9d).

The points up to 207.09 kNm^2 were detected in the closed volume of the building's northern façade (Fig. 10a), and these stresses caused small cracks in the middle of this façade, which were attempted to be repaired (Fig. 10b).

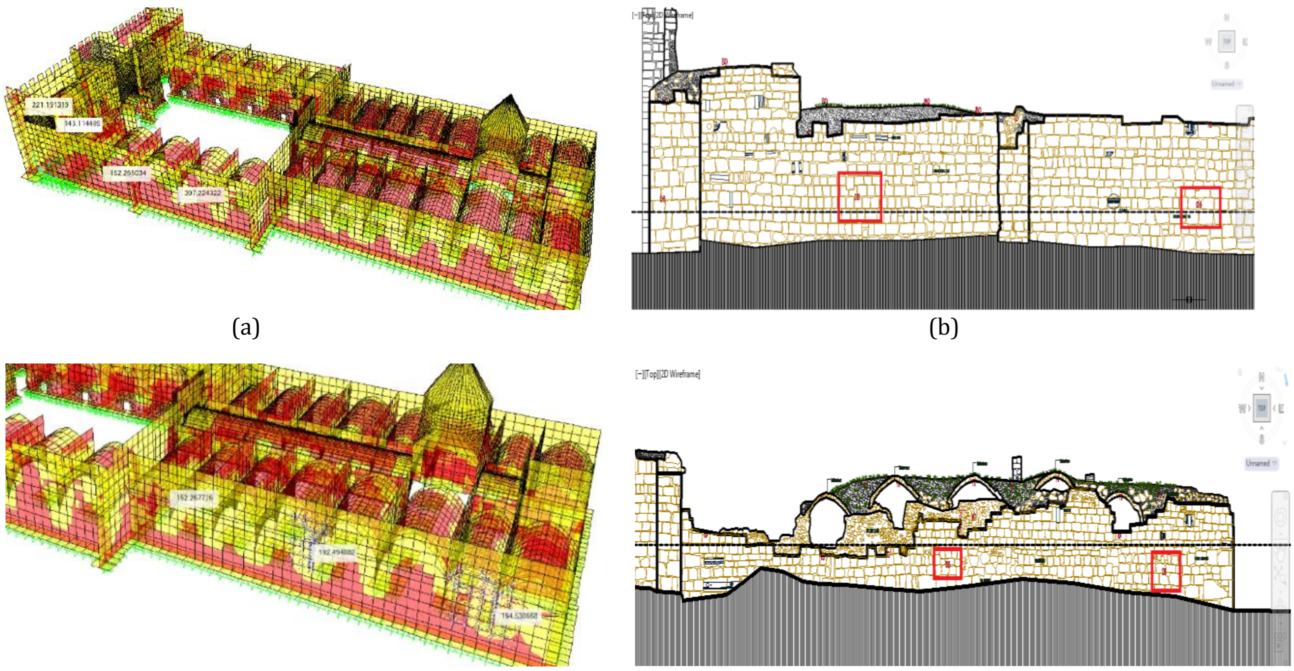

(a) (b)

(a) (b)

Fig. 9. Historical Obruk Inn: (a) South facade maximum stress distribution under vertical loads; (b) South facade laser scanning result; (c) Outer facade closed volume maximum stress distribution under vertical loads; (d) South facade closed volume laser scanning result.

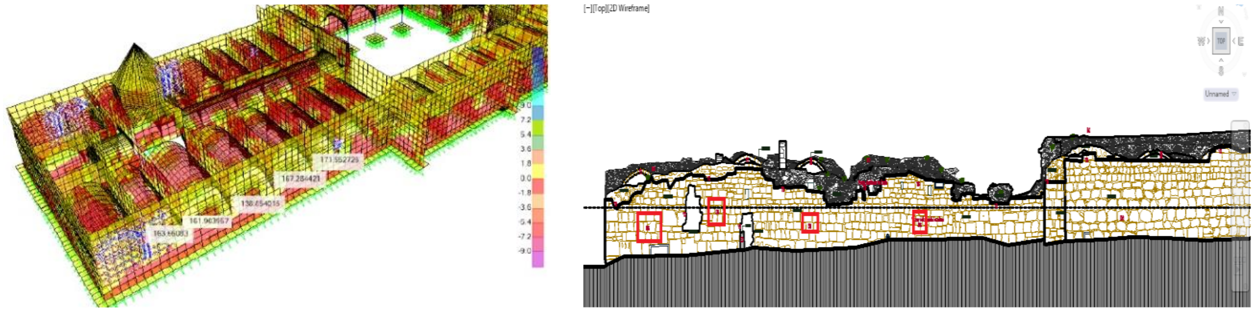

(a) (b)

Fig. 10. Historical Obruk Inn: (a) North facade maximum stress distribution under vertical loads; (b) North facade laser scanning result.

Base shear forces and displacements obtained by the time history analysis are given in Fig. 11. The compressive and tensile stresses occurred in the vaults as a result of the earthquake acceleration records applied are given in Fig. 12.

Under the influence of earthquakes, the vaults in the structure suffer significant strains. Individual stress distributions for each earthquake record are given in Fig. 13.

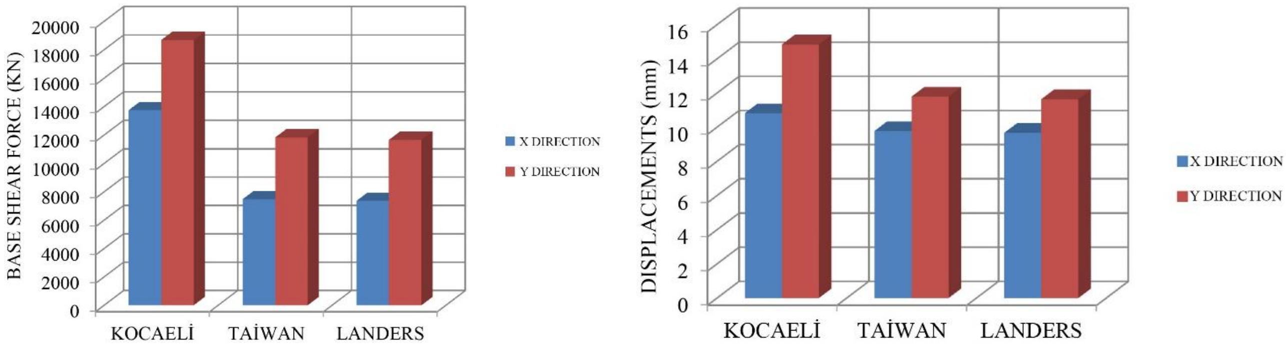

(a) (b)

Fig. 11. Time history analysis of historical Obruk Inn: (a) Base shear force; (b) Displacement.

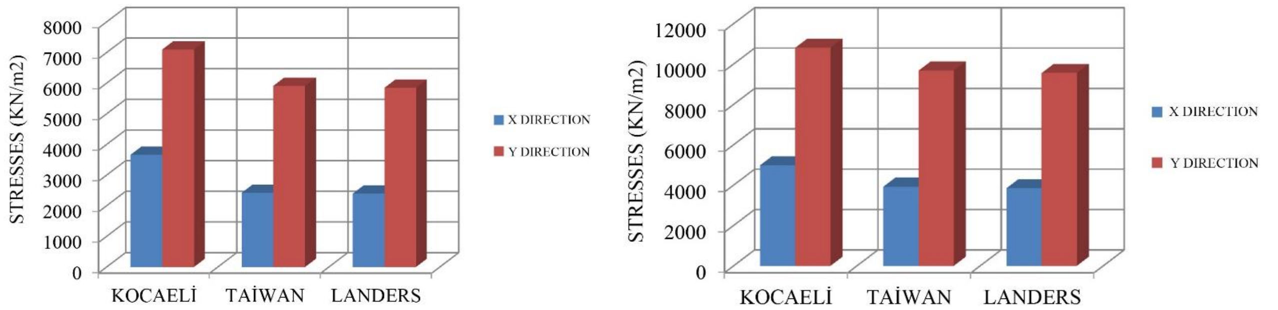

(a) (b)

Fig. 12. Time history analysis of historical Obruk Inn: (a) Tensile stresses in vault; (b) Compressive stresses in vault.

4. Conclusions

It is important to preserve historic buildings. The aim of this study is to understand the structural performance of historic masonry building. Obtained results of FEM analysis corrected the structural damage pattern of the existing building. The precautions should be taken immediately to preserve the building. Valid strengthening technics are being used for a long time.

Alhoubi et al. (2022) investigated the effectiveness of FRCM reinforcement in confining the columns and had Test results showed that confining the pre-damaged columns with PBO–FRCM systems resulted in 7–42% enhancement in their load-carrying capacity and 47–272% improvement in their ductility.

Tello et al. (2021) tested 12 short columns under axial compression, PBO-FRCM systems enhanced the capacity of columns. Columns strengthened with two and four PBO-FRCM layers showed a gain in the capacity of up to 40% and 75%, respectively.

Tello et al. (2023) had tested 4 rectangular and 4 circular columns under concentric loading. For each type of cross-section, columns were wrapped with 1, 2 or 4 layers of PBO FRCM. Overall, the strengthened columns exhibited higher load carrying capacity than their control unwrapped counterpart with an increase ranged between 5.1% and 36%.

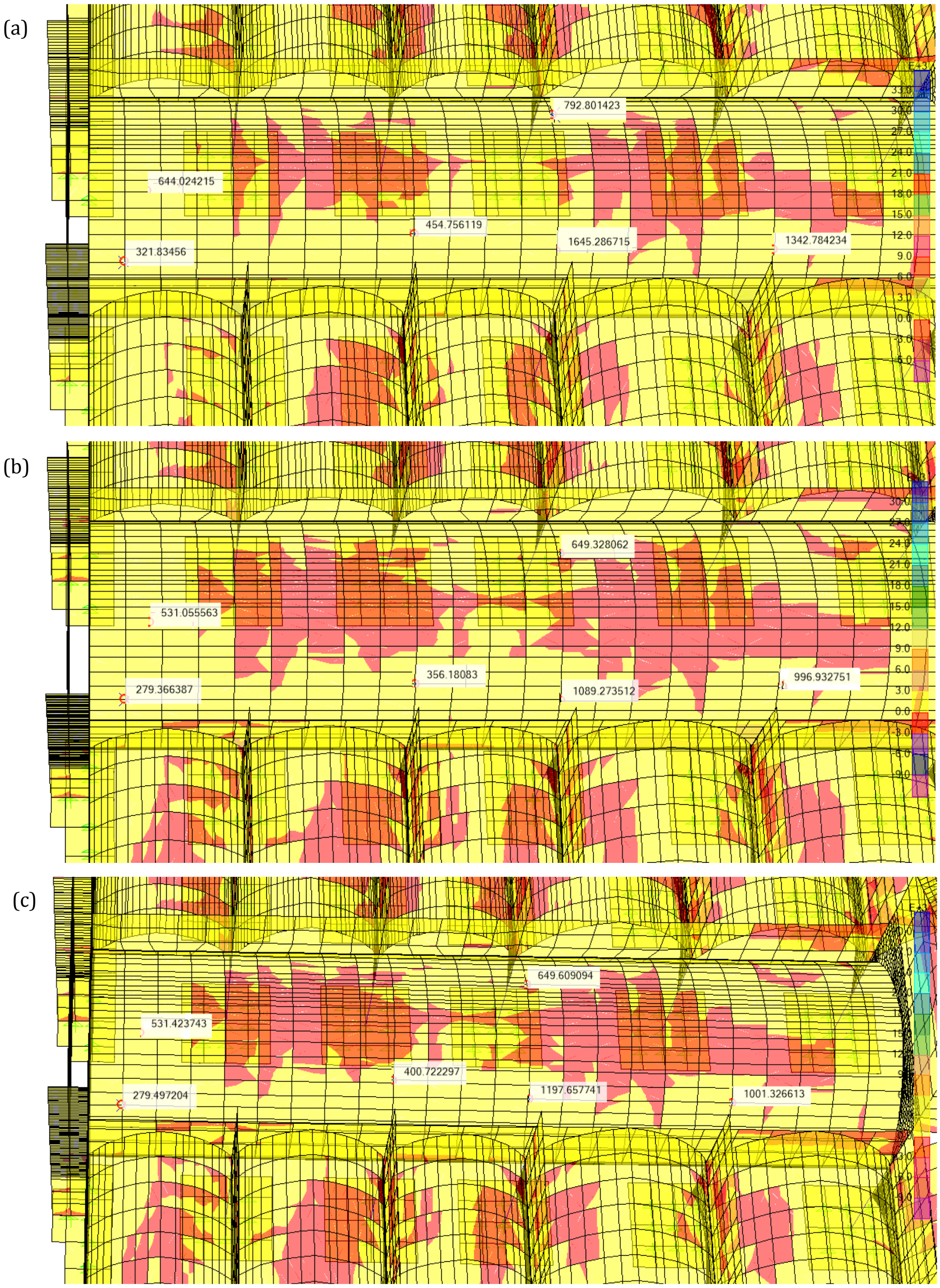

Fig. 13. Stresses in the vaults under the influence of earthquakes: (a) Kocaeli; (b) Lander; (c) Taiwan.

Kyaure and Abed (2021) studied a three-dimensional (3D) nonlinear finite element (FE) model and developed using ABAQUS to study the behavior of corrosion damaged RC columns retrofitted with poly-paraphenylene-ben-zobisoxazole (PBO) FRCM systems. Geometric and material nonlinearities in concrete, cement mortar and composite are incorporated in the FE model that is validated through axial capacity and failure mode comparisons against published literature.

The structural performance of the historical Obruk Inn under the influence of vertical and earthquake loads. was investigated in this work. The obtained results give ideas about the parts of the structure while strengthening. The following findings were obtained as a result of the study:

- High stresses exceeding the safety stress in the horizontal and vertical directions cause cracks in walls, vaults, arches, and other building elements, material losses, melting of materials, joint discharge, and many other problems.
- The highest strains in the structure were found at the vault and arches' supports, as well as at the upper

points of arches. While restoration newly strengthening methods should be used to preserve structural damages. Excessive deformation, particularly in the vault and arch parts of the structure, may result in sudden collapse.
- Analysis had showed that the stress and displacement values occurred by the Kocaeli earthquake records are greater than the maximum stress and displacement values occurred according to the Landers and Taiwan earthquake records. This is concluded because of the high base shear.
- The stress and displacement results from the Landers and Taiwan earthquake records are comparable.
- The structure should be strengthened immediately to prevent further damage from stresses caused by vertical loads.

Acknowledgements

None declared.

Funding

The authors received no financial support for the research, authorship, and/or publication of this manuscript.

Conflict of Interest

The authors declared no potential conflicts of interest with respect to the research, authorship, and/or publication of this manuscript.

Author Contributions

All of the authors made substantial contributions to conception and design, or acquisition of data, or analysis and interpretation of data; were involved in drafting the manuscript or revising it critically for important intellectual content; and gave final approval of the version to be published.

Data Availability

The datasets created and/or analyzed during the current study are not publicly available, but are available from the corresponding author upon reasonable request.

REFERENCES

Abruzzese D, Miccoli L, Yuan J (2009). Mechanical behavior of leaning masonry Huzhu Pagoda. *Journal of Cultural Heritage*, 10 (2009) 480–486.

Ahmadzai E, Yaman Z, Cumhur A (2022). Experimental examination of strength and behavior of masonry brick walls strengthened with expanded steel plates. *Challenge Journal of Structural Mechanics,* 8(3), 110-121.

Akcay C, Bozkurt TS, Sayin B, Yildizlar B (2016). Seismic retrofitting of the historical masonry structures using numerical approach. *Construction and Building Materials*, 113, 752–763.

Alhoubi Y, El Refai A, Abed F, El-Maaddawy T, Tello N (2022). Strengthening pre-damaged RC square columns with fabric-reinforced cementitious matrix (FRCM): Experimental investigation. *Composite Structures*, 294, 115784.

Asteris PG, Chronopoulos MP, Chrysostomou CZ, Varum H, Plevris V, Kyriakides N, Silva V (2015). Seismic vulnerability assessment of historical masonry structural systems. *Engineering Structures*, 62–63, 118–134.

Aşıkoğlu A, Vasconcelos G, Lourenço PB, Pantò B (2020). Pushover analysis of unreinforced irregular masonry buildings: Lessons from different modeling approaches. *Engineering Structures*, 218, 110830.

Bruneau M (1994). State-of-the-art report on seismic performance of unreinforced masonry buildings. *Journal of Structural Engineering*, 120.

Cakir F (2022). Performance-based assessment of long masonry structures. *Challenge Journal of Structural Mechanics*, 8(2), 47-56.

Chen SY, Moon FL, Yi T (2008). A macroelement for the nonlinear analysis of in-plane unreinforced masonry piers. *Engineering Structures*, 30, 2242–2252.

D'Agostino S, Lombardi G, Russo G, Viggiani C (2010). Structural engineering and geology applied to the static problems of the Etruscan "Tomba dell'Orco" (Tarquinia, Central Italy). *Journal of Cultural Heritage*, 11, 107–112.

Eslami A, Ronagh HR, Mahini SS, Morshed R (2012). Experimental investigation and nonlinear FE analysis of historical masonry buildings – A case study. *Construction and Building Materials*, 35, 251-260.

Gattesco N, Macorini L (2014). In-plane stiffening techniques with nail plates or CFRP strips for timber floors in historical masonry buildings. *Construction and Building Materials*, 58, 64–76.

Giordano A, Mele E, De Luca A (2002). Modelling of historical masonry structures: Comparison of different approaches through a case study. *Engineering Structures*, 24, 1057–1069.

Grillanda N, Chiozzi A, Bondi F, Tralli A, Manconi F, Stochino F, Cazzani A (2019). Numerical insights on the structural assessment of historical masonry stellar vaults: the case of Santa Maria del Monte in Cagliari. *Continuum Mechanics and Thermodynamics*, 1–24.

Hamid AA (2006). How to Face The Increasing Cost of Reinforcing Steel in RC Frame Construction in Egypt. Keynote Lecture, In: *Workshop of Proposed Alternatives to Face the Increasing Cost of Steel Reinforcement Used in RC Structures in Egypt*, Cairo, Egypt.

Hejazi M, Hejazi B, Hejazi S (2015). Evolution of Persian traditional architecture through the history. *Journal of Architecture and Urbanism*, 39, 188–206.

Hejazi M, Pourabedin M (2021). Performance of persian brick masonry discontinuous double-shell domes against earthquakes. *Engineering Failure Analysis*, 119, 104994.

Kamal OA, Hamdy GA, El-Salakawy TS (2014). Nonlinear analysis of historic and contemporary vaulted masonry assemblages. *HBRC Journal*, 10, 235–246.

Karaton M, Çanakçı K (2021). Yığma duvarların mikro modellemesinde harcın çekme dayanımı ve kayma gerilmesi iletim katsayısının çözümler üzerindeki etkisinin incelenmesi. *Dicle Üniversitesi Mühendislik Fakültesi Mühendislik Dergisi*, 12(1), 175-185. (in Turkish)

Klinger RE (2010). Masonry Structural Design. 1st ed., McGraw-Hill Professional.

Kollerathu JA, Menon A (2017). Role of diaphragm flexibility modelling in seismic analysis of existing masonry structures. *Structures*, 11, 22–39.

Kujawa M, Lubowiecka I, Szymczak C (2020). Finite element modelling of a historic church structure in the context of a masonry damage analysis. *Engineering Failure Analysis*, 107, 104233.

Kyaure M, Abed F (2021). Finite element parametric analysis of RC columns strengthened with FRCM. *Composite Structures*, 275, 114498.

Laefer DF, Truong-Hong L, Carr H, Singh M (2014). Crack detection limits in unit based masonry with terrestrial laser scanning. *NDT & E International*, 62, 66–76.

Lourenço PB (1996). Computational Strategies for Masonry Structures. *Ph.D. thesis*, Delft University, Delft, Netherlands.

Milani G, Shehu R, Valente M (2017). Possibilities and limitations of innovative retrofitting for masonry churches: Advanced computations on three case studies. *Construction and Building Materials*, 147, 239–263.

Pauletta M, Di Luca D, Russo E, Fumo C (2018). Seismic rehabilitation of cultural heritage masonry buildings with unbonded fiber reinforced elastomeric isolators (U-FREIs) – A case of study. *Journal of Cultural Heritage*, 32, 84–97.

Petrovčič S, Kilar V (2013). Seismic failure mode interaction for the equivalent frame modeling of unreinforced masonry structures. *Engineering Structures*, 54, 9–22.

Sandoli A, Musella C, Piero Lignola G, Calderoni B, Prota A (2020). Spandrel panels in masonry buildings: Effectiveness of the diagonal strut model within the equivalent frame model. *Structures*, 27, 879–893.

Tello N, Alhoubi Y, Abed F, El Refai A, El-Maaddawy T (2021). Circular and square columns strengthened with FRCM under concentric load. *Composite Structures*, 255, 113000.
Tello N, Farid A, El Refai A, El-Maaddawy T, Alhoubi Y (2023). Experimental investigation of pre-damaged circular RC columns strengthened with fabric-reinforced cementitious matrix (FRCM). *Structural Concrete*, 24, 1464-4177.
Theodossopoulos D, Sinha B (2013). A review of analytical methods in the current design processes and assessment of performance of masonry structures. *Construction and Building Materials*, 41, 990–1001.
Tomazevic M (1999). Earthquake-Resistant Design of Masonry Buildings. Imperial College Press.
Tomaszewska A (2010). Influence of statistical errors on damage detection based on structural flexibility and mode shape curvature. *Computers & Structures*, 88, 154–164.
Tomaszewska A, Szymczak C (2012). Identification of the Vistula Mounting tower model using measured modal data. *Engineering Structures*, 42, 342–348.
TEC-2007 (2007). Specifications for buildings to be built in seismic areas. Turkish Earthquake Code, Ankara, Türkiye.
TS-498 (1997). Design Loads for Buildings. Turkish Standard Institute, Ankara, Türkiye.
Uzun M, Korkmaz HH (2018). Investigation of numerical analysis according to two different methods of an existing masonry building, *Journal of Engineering Research and Applied Science*, 7, 965–971.